Compact, robust, and flexible setup for femtosecond pulse shaping

A. Präkelt, M. Wollenhaupt, A. Assion, Ch. Horn, C. Sarpe-Tudoran, M. Winter, and T. Baumert[a)]
Universität Kassel, Institut für Physik und Center for Interdisciplinary Nanostructure Science and Technology (CINSaT), Heinrich-Plett-Str. 40, D-34132 Kassel, Germany

(Received 2 July 2003; accepted 28 July 2003)

We present an improved design and adjustment concept for femtosecond pulse shaping. The concept results in a compact and robust pulse shaping setup. A systematic adjustment procedure, high reproducibility and stability, as well as easy adaptability to different femtosecond laser sources are the key features of the presented design. The constructed prototype pulse shaper was tested in an open loop and feedback-controlled adaptive pulse shaping on two different femtosecond laser sources. © *2003 American Institute of Physics.* [DOI: 10.1063/1.1611998]

Femtosecond pulse shaping techniques have an impact on an increasing number of scientists in physics, chemistry, biology, and engineering. This is due to the fact that primary light-induced processes can be studied and even actively controlled if ultrashort shaped laser pulses are available. Femtosecond laser pulse shaping techniques using spatial light modulators (SLMs) were recently reviewed by Weiner.[1] In that work, liquid crystals (LCs), acousto-optic elements as well as moving and deformable mirrors are discussed as SLMs. A review focusing on acousto-optic elements was given in Ref. 2. Implementing these devices in a feedback loop allows for adaptive femtosecond pulse shaping demonstrated on an automated pulse compression of ultrashort light pulses[3,4] and on the control of chemical reactions.[5,6] In the meantime, these techniques have found many applications in different fields of science and engineering (see, for example, Refs. 7 and 8). In this Note, we report on a design and adjustment concept for a compact and robust pulse shaper setup. It meets the demands for ''user friendliness'' that are systematic adjustability, high reproducibility, and stability, and easy adaptability to multiple laser sources. Our setup is realized on a kHz Ti:Sapphire amplifier system [30 fs full width at half maximum (FWHM) pulse duration, 0.8 mJ pulse energy, and 750 to 835 nm spectral pedestal width, i.e., full width at 10% of maximum spectral intensity] and a Ti:Sapphire femtosecond oscillator (10 fs FWHM pulse duration, 5 nJ pulse energy, and 700 to 900 nm spectral pedestal width). However, the described design rules are general and can be adapted to the available SLM and the specific femtosecond laser source. We chose a LC-SLM for the demonstration of our concept because of its independence of the pulse repetition rate and its inherently high efficiency.[1] Moreover, recent LC technology has extended the number of pixels from 128 [at Cambridge Research and Instrumentation Inc. (CRI) Woburn, MA, SLM-128 used in this Note] to 640.[9] This article is organized as follows. First, a short introduction into Fourier transform pulse shapers will be given. Then, we will describe our concept for building such a device. In that part, we will discuss several design types for Fourier transform pulse shapers and present our setup including construction issues and the adjustment principle. Finally, we describe a number of tests which were performed to certify the performance of the constructed pulse shaper.

Because of their short duration, femtosecond laser pulses cannot be directly shaped in the time domain. Therefore, the idea of pulse shaping is modulating the incident spectral electric field $\tilde{E}_{\mathrm{in}}(\omega)$ by a (linear) mask $\tilde{M}(\omega)$ in frequency domain. This results in an outgoing shaped spectral electric field $\tilde{E}_{\mathrm{out}}(\omega)$:

$$\tilde{E}_{\mathrm{out}}(\omega)=\tilde{M}(\omega)\tilde{E}_{\mathrm{in}}(\omega). \tag{1}$$

The mask may modulate the spectral amplitude $\tilde{A}(\omega)$ and phase $\Delta\varphi(\omega)$, i.e., $\tilde{M}(\omega)=\tilde{A}(\omega)\exp[i\Delta\varphi(\omega)]$. Furthermore, polarization shaping has been demonstrated.[10]

One way to realize a pulse shaper is the Fourier transform pulse shaper which uses a SLM as a mask. Its operation principle is based on optical Fourier transformations from the time domain into the frequency domain and vice versa. In Fig. 1(a), a standard design of such a pulse shaper is sketched. The incoming ultrashort laser pulse is dispersed by a grating and the spectral components are focused by a lens of focal length f. In the back focal plane of this lens—the Fourier plane—the spectral components of the original pulse are separated from each other having minimum beam waists. By this means, the spectral components can be modulated individually by placing a SLM into the Fourier plane. Afterwards, the short laser pulse is reconstructed by performing an inverse Fourier transformation back into the time domain. Optically, this is realized by a mirrored setup consisting of an identical lens and grating. The whole setup—without the SLM—is called a zero-dispersion compressor since it introduces no dispersion if the $4f$ condition is met.[11] As a part of such a zero-dispersion compressor, the lenses separated by the distance $2f$ form a telescope with unitary magnification. Spectral modulations as stated by Eq. (1) can be set by the SLM.

Commonly, pulse shapers are constructed using commercial standard optomechanical components. In addition, some

a)Electronic mail: baumert@physik.uni-kassel.de

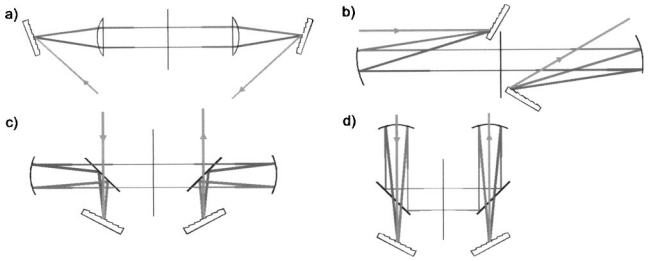

FIG. 1. Top views of different design types for pulse shapers based on an optical Fourier transformation.

dedicated designs using microfabrication techniques for fixed mask and mechanical antireflection switches have been reported.[12,13] As pulse shapers consist of a significant amount of degrees of freedom, we chose a different approach and constructed an integrated custom-made design. The idea is to eliminate many degrees of freedom by precise mechanical manufacturing and then iteratively adjust the remaining degrees of freedom in a step-by-step procedure. Furthermore, all optical components can be reproducibly removed and repositioned within the pulse shaper using mechanical fits.

In Fig. 1, different types of Fourier transform pulse shapers are presented. Since the damage threshold of a pulse shaper is limited by the damage threshold of the active area of the LC-SLM, cylindrical focusing lenses or mirrors are preferable to spherical optics for all design types. Design type a is the standard design. This design has the advantage that all optical components are positioned along an optical axis. Due to chromatic abberations, temporal and spatial reconstruction errors are introduced through the lenses. This limits the applicability of type a to pulses with pulse durations around 100 fs and above. Therefore, the lenses are replaced by curved mirrors (types b–d). In general, optical errors are minimized if the tilting angles of the curved mirrors within the telescope are as small as possible.

In design type b, all optical components are in a horizontal plane. The tilt between the curved mirror and the grating complicates the implementation of type b into an integrated design. The active area of a one-dimensional LC-SLM has a larger width than height (e.g., 12.8×2.0 mm for the CRI SLM-128/256 and 63.7×7.0 mm for the Jenoptik AG (Jena, Germany) SLM-S 640/12) implying a larger beam width than height in the Fourier plane. Therefore, smaller tilting angles are achieved by introducing the tilt of the curved mirrors in the vertical direction. Design types c and d make use of vertical beam steering with two plane mirrors for folding the beam. In type c, the incoming beam travels above this folding mirror, impinges on the grating, and is dispersed into its spectral components. Because of the tilt of the grating in the vertical direction, the spectral components are deflected downward. Then, they are reflected by the folding mirror onto the cylindrical mirror and sagitally focused into the Fourier plane, modulated by the SLM, and inversely Fourier transformed back by a mirrored setup. In type d, the position of the curved and folding mirrors are exchanged. Types c and d allow very small tilting angles of the curved mirrors at the order of 1°. Another advantage of both design types is that the gratings are placed in quasi-Littrow configuration. For our compact design, d was chosen over c because of the better accessibility of the adjustment screws.

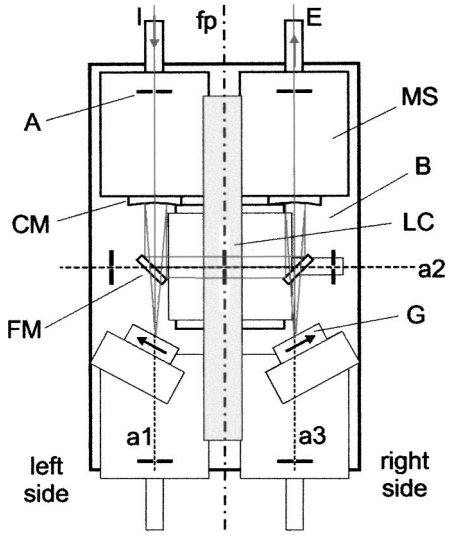

FIG. 2. Sketch of built pulse shaper (top view, size: 130×200 mm^2). The whole setup is mounted on a base plate (B) with micropositioning stages (MS) for important degrees of freedom. The incoming beam (I) enters the pulse shaper on the left-hand side along axis 1 (a1) and is dispersed by the first grating (G) (blaze arrows are plotted). The spectral components go downward and are sagitally focused by a cylindrical mirror (CM). After reflection on a plane folding mirror (FM), they travel along axis 2 (a2) with sagittal foci in the Fourier plane (fp). Then, the original beam is reconstructed by a mirrored setup and exits (E) the pulse shaper on the right-hand side travelling along axis 3 (a3). The LC-SLM (LC) is placed directly along the Fourier plane. Not all of the apertures (A) used for adjustment can be seen in the sketch.

A sketch of the constructed integrated design is depicted in Fig. 2. A mechanical precision of 0.1 mm was chosen for the construction. At first, the Fourier plane (see fp in Fig. 2) was defined in the center of the base plate. At this position, either the LC-SLM (see LC in Fig. 2) or a screen and an aperture for beam adjustment can be placed. The pulse shaper was constructed around the Fourier plane and the LC-SLM. All components are mounted on top of the base plate (see B in Fig. 2). At the lowest level on the base plate, micropositioning stages (see MS in Fig. 2) are mounted to adjust the optical components according to the $4f$ condition. The optical components (gratings, curved mirrors, and folding mirrors) are fixed on mirror mounts via specific adapters. Each mirror mount is fixed on a micropositioning stage via two adapters—the lower one having interference fits, the upper one clearance fits. For a further description see the corresponding caption of Fig. 2.

The height of the active area of the LC-SLM determines the diameter of the beam in front of the pulse shaper, i.e., 2 mm for the CRI SLM-128. The required polarization for the incoming beam is specified by the manufacturer of the LC-SLM—in our case, horizontal polarization. The focal length 75.7 mm of the cylindrical mirrors was chosen so that the sagittal beam waists in the Fourier plane roughly match the size of a single pixel of the LC-SLM (0.1 mm). Within the usable spectral width of the LC-SLM, only the selection of the gratings critically depends on the laser source. For a given focal length, the groove frequencies of the gratings were chosen to illuminate the active area of the LC-SLM

taking the spectral pedestal width of the laser source into account. Different gratings for different laser sources can be put onto several upper adapters with clearance fits and can, therefore, be reproducibly exchanged. In this way, the pulse shaper can be easily adapted to multiple laser sources. For example, for the 30 fs Ti:Sapphire amplifier with a spectral pedestal width from 750 to 835 nm, we chose gratings with 1200 grooves/mm; while for the 10 fs Ti:Sapphire oscillator with the spectral pedestal width from 700 to 900 nm, gratings with a groove frequency of 830.8 grooves/mm were selected. The efficiencies of the gratings mainly determine the total energy throughput of the pulse shaper, e.g., in the case of the amplifier gratings, 55%. Taking the reflectivity of specially designed compressor gratings into account, a total energy throughput of higher than 70% is estimated.

We incorporated several removable apertures (see A in Fig. 2) into our design at well defined positions in order to assure a correct and systematic alignment. A principle adjustment procedure for pulse shapers of type a is given in Ref. 1. For our setup, the adjustment procedure is somewhat different. It consists of two separate parts: the ''geometric'' and the ''femtosecond'' alignments. The objective of the first procedure is the adjustment of the telescope while the femtosecond alignment pursues the final adjustment including the temporal and spatial beam reconstruction. A He–Ne laser is sufficient for the geometric adjustment. First, the folding mirrors (see FM in Fig. 2) as well as the cylindrical mirrors (see CM in Fig. 2) are adjusted by the corresponding apertures. Within this adjustment step, the folding mirrors are removed and reversibly repositioned. The $2f$ condition of the telescope is achieved via tuning the micropositioning stages (see MS in Fig. 2) below the cylindrical mirrors so that parallel incoming beams are focused on the screen in the Fourier plane. Furthermore, at the position of the gratings (see G in Fig. 2), plane mirrors can be mounted for the simulation of the beam path of the He–Ne laser through the whole setup. After the geometric adjustment, the first step of the femtosecond alignment is checking the telescope using the femtosecond laser source. This source is optically adapted to the pulse shaper with respect to beam diameter in front of the pulse shaper. For the subsequent femtosecond adjustment, we use web cams or an IR viewer to monitor our near-IR (NIR)-laser beams. First, the appropriate gratings are mounted at their positions (see G in Fig. 2). Then, the gratings are put into a real Littrow configuration for the central frequency of horizontal beams passing along axes one and three (see a1 and a3 in Fig. 2). The gratings are adjusted so that all of the diffractive orders are on the same height above the optical table. Next, the first grating is tilted downward so that the spectrum matches the predefined position on the screen in the Fourier plane. The second grating is tilted in the same way to reconstruct the incoming beam. The alignment is checked by comparison of the reconstructed (see E in Fig. 2) and the original beam profiles (see I in Fig. 2) at different distances after the pulse shaper. Specifically, the spatial chirp is investigated. Besides blocking frequency components by introducing an obstacle into the Fourier plane, the spatial chirp of NIR sources can be observed by using a web cam which discriminates bluer and redder components from each other. An advantage of our integrated design is that the spatial reconstruction is already accomplished by the beam path predefined by reproducibly exchangeable optical components and the precise alignment by the apertures.

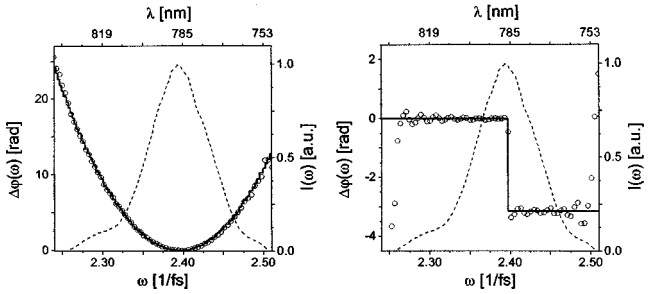

FIG. 3. Two examples of phase modulation introduced by the pulse shaper: Quadratic phase modulation $[\Delta\varphi(\omega)=1000\ \mathrm{fs}^2(\omega-2.397\ \mathrm{fs}^{-1})^2]$ on the left-hand side, π-jump phase modulation on the right-hand side. The straight black lines are the desired phase modulations while the small circles were measured by spectral interferometry. For comparison, the spectral intensity $I(\omega)$ of the used Ti:Sapphire amplifier is plotted as a dashed line.

The temporal reconstruction, i.e., the exact position of the gratings to guarantee the $4f$ condition, requires a femtosecond pulse characterization tool for the existing beam. For this purpose, we place the pulse shaper into one arm of a Mach-Zehnder interferometer with a delay line in the other arm. To characterize the pulse, we use the following techniques: (i) a second-harmonic signal, (ii) a frequency-resolved optical gating (FROG),[14,15] (iii) spatial spectral interferometry (SSI),[16] and (iv) spectral interferometry (SI).[17,18] By iteratively checking the temporal and spatial reconstruction, the gratings are aligned into their correct position. Finally, the LC-SLM is inserted into the setup at its predefined position. Due to the mechanical precision, the wavelength calibration, i.e., ''wavelength versus pixel number,'' is accurate to within one pixel at the predefined position of the LC-SLM. Thus, micropositioning stages for the LC-SLM are optional. The wavelength calibration completes the adjustment of the pulse shaper. Because of the high mechanical stability of our design, readjustment is not necessary. The laser beam has to be correctly coupled into the pulse shaper setup using the corresponding apertures. If gratings, which are mounted on top of an adapter with clearance fits, are adjusted once for a specific source, they can be exchanged without readjustment. This has been verified for our amplifier and oscillator gratings. In combination with our detailed step-by-step adjustment procedure, this makes our pulse shaper very user friendly.

In order to check the performance of our device, several standard tests were carried out. For higher accuracy, the birefringence dispersion of the LCs is taken into account within the modulation setting program. The applied CRI SLM-128 is a phase-only modulator. The fidelity of our phase modulator was investigated using SSI, FROG, and SI. In Fig. 3, the results of two measurements using the amplifier are plotted showing good agreement between the desired and the phase modulation measured by SI. The oscillations at the π-jump modulation are created during the phase retrieval due to the spectral resolution of the used spectrometer. In addition, the modulation of the spatial beam profile, depen-

dent on the set modulation, was checked with a charge coupled device matrix. We observed a quarter of a millimeter parallel spatial shift per picosecond pulse duration which is in agreement with the theoretical predictions.[19] Furthermore, we performed adaptive pulse shaping experiments employing a feedback loop and an optimization algorithm. The standard second-harmonic generation signal, to adaptively compress the pulse,[3,4] and other less common signals were successfully used. In these test runs, voltages per pixels as well as certain parameters, like the group delay dispersion, were used as genes of the evolutionary algorithm.[7]

Concluding, we have presented the design, construction, and adjustment concept for compact rugged pulse shapers which delivers high precision, long-term stability, user friendliness, and easy adaptability to the given laser source. The precise design and manufacturing featuring exchangeable optical components and apertures by mechanical fits allow a straightforward, precise, and logic adjustment. This significantly relieves the work of the experimentalist and makes transferability to other users and laboratories much easier. By a set of test runs, the design concept was successfully demonstrated using a CRI SLM-128 as the LC-SLM and two Ti:Sapphire lasers as sources.

Support of the Deutsche Forschungsgemeinschaft and the Fonds der Chemischen Industrie is gratefully acknowledged.

[1] A. M. Weiner, Rev. Sci. Instrum. **71**, 1929 (2000).
[2] M. A. Dugan, J. X. Tull, and W. S. Warren, in *Advances in Magnetic and Optical Resonance*, edited by W. S. Warren (Academic, New York, 1997), Vol. 20.
[3] T. Baumert, T. Brixner, V. Seyfried, M. Strehle, and G. Gerber, Appl. Phys. B: Lasers Opt. **65**, 779 (1997).
[4] D. Yelin, D. Meshulach, and Y. Silberberg, Opt. Lett. **22**, 1793 (1997).
[5] A. Assion, T. Baumert, M. Bergt, T. Brixner, B. Kiefer, V. Seyfried, M. Strehle, and G. Gerber, Science **282**, 919 (1998).
[6] C. J. Bardeen, V. V. Yakovlev, K. R. Wilson, S. D. Carpenter, P. M. Weber, and W. S. Warren, Chem. Phys. Lett. **280**, 151 (1997).
[7] T. Brixner, N. H. Damrauer, and G. Gerber, in *Advances in Atomic Molecular and Optical Physics*, edited by H. Walther (Academic, San Diego, 2001), Vol. 46.
[8] D. Goswami, Phys. Rep. **374**, 385 (2003).
[9] G. Stobrawa, M. Hacker, T. Feurer, D. Zeidler, M. Motzkus, and F. Reichel, Appl. Phys. B: Lasers Opt. **72**, 627 (2001).
[10] T. Brixner and G. Gerber, Opt. Lett. **26**, 557 (2001).
[11] O. E. Martinez, IEEE J. Quantum Electron. **24**, 2530 (1988).
[12] R. Grote and H. Fouckhardt, Opt. Express **4**, 328 (1999).
[13] J. E. Ford and J. A. Walker, IEEE Photonics Technol. Lett. **10**, 1440 (1998).
[14] R. Trebino, K. W. DeLong, D. N. Fittinghoff, J. N. Sweetser, M. A. Krumbügel, B. A. Richman, and D. J. Kane, Rev. Sci. Instrum. **68**, 3277 (1997).
[15] R. Trebino, *Frequency-Resolved Optical Gating: The Measurement of Ultrashort Laser Pulses* (Kluwer, Norwell, MA, 2000).
[16] D. Meshulach, D. Yelin, and Y. Silberberg, J. Opt. Soc. Am. B **14**, 2095 (1997).
[17] L. Lepetit, G. Chériaux, and M. Joffre, J. Opt. Soc. Am. B **12**, 2467 (1995).
[18] C. Dorrer, N. Belabas, J.-P. Likforman, and M. Joffre, J. Opt. Soc. Am. B **17**, 1795 (2000).
[19] M. M. Wefers and K. A. Nelson, IEEE J. Quantum Electron. **32**, 161 (1996).